

# Skyrmion-mediated Nonvolatile Ternary Memory

<sup>1</sup>Md Mahadi Rajib, <sup>3</sup>Namita Bindal, <sup>3</sup>Ravish Kumar Raj, <sup>3</sup>Brajesh Kumar Kaushik and <sup>1,2</sup>Jayasimha Atulasimha

<sup>1</sup>Department of Mechanical and Nuclear Engineering, Virginia Commonwealth University, Richmond, VA 23284, USA

<sup>2</sup>Department of Electrical and Computer Engineering, Virginia Commonwealth University, Richmond, VA 23284, USA

<sup>3</sup>Department of Electronics and Communication Engineering, Indian Institute of Technology Roorkee, Roorkee, Uttarakhand 247667, India

## Abstract

Multistate memory systems have the ability to store and process more data in the same physical space as binary memory systems, making them a potential alternative to existing binary memory systems. In the past, it has been demonstrated that voltage-controlled magnetic anisotropy (VCMA) based writing is highly energy-efficient compared to other writing methods used in non-volatile nano-magnetic binary memory systems. In this study, we introduce a new, VCMA-based and skyrmion-mediated non-volatile ternary memory system using a perpendicular magnetic tunnel junction (p-MTJ) in the presence of room temperature thermal perturbation. We have also shown that ternary states  $\{-1, 0, +1\}$  can be implemented with three magnetoresistance values obtained from a p-MTJ corresponding to ferromagnetic up, down, and skyrmion state, with 99% switching probability in the presence of room temperature thermal noise in an energy-efficient way, requiring  $\sim 3$  fJ energy on an average for each switching operation. Additionally, we show that our proposed ternary memory demonstrates an improvement in area and energy by at least 2X and  $\sim 60$ X respectively, compared to state-of-the-art spin-transfer torque (STT)-based non-volatile magnetic multistate memories. Furthermore, these three states can be potentially utilized for energy-efficient, high-density in-memory quantized deep neural network implementation.

## Introduction

In the field of computer technology, CMOS-based two-state memory is widely used. When evaluating memory systems, key considerations include writing and reading speed, reliability, endurance, non-volatility, high density, and energy-efficiency [1]. As CMOS-based two-state memory systems are volatile and are reaching their limits for high-density implementation, researchers are searching for alternatives. Currently, flash memory is the most advanced non-volatile option available, however, it has an endurance problem [1-3]. Other potential options that are still being researched include resistive random-access-memory (RRAM) [4] phase change memory (PCM) [5] magnetoresistive random-access memory (MRAM) [6, 7] and ferroelectric random-access memory (FeRAM) [8, 9] with MRAM being the most promising [1, 10]. MRAM devices are made up of nanomagnets, where the "up" and "down" states typically represent the "0" and "1" bits in a p-MTJ as shown in Fig. 1(a). There are two main methods to write these bits, a current-dependent method [11-14] and an electric field-dependent method [15-19]. The current-dependent approach typically results in high energy dissipation when switched with STT [11,12,20]. Using spin-orbit torque (SOT) could potentially improve energy-efficiency, however, it requires a three terminal device geometry [13]. On the other hand, electric field-based write approach can be more energy-efficient whether mediated through strain [21-27] or voltage control of magnetic anisotropy [17, 28, 29] or other methods such as electrical switching of polarization coupled to antiferromagnetic state [30]. In particular, MTJs switched with strain can potentially be scaled to switch at  $< 1$  fJ/bit [31] while voltage-controlled magnetic

anisotropy-based switching, a type of electric field-dependent method, requires only a few fJ [32, 33] of energy per switching operation compared to 100 fJ using STT switching (a current-dependent method) [34]. Along with energy-efficiency high density of RAMs is also desirable, so a multi-state approach is more practical. In the past, multistate MRAM has been proposed using STT [35] and SOT [36], but these methods result in decreased density because they involve connecting MTJs in parallel or series. Three-terminal devices like spin-orbit torque magnetic random-access-memory (SOT-MRAM) require more space, and multibit spin-transfer torque magnetic random-access-memory (STT-MRAM) requires even more energy than its two-state counterpart. Therefore, there is a need to implement a multibit memory system in a single MTJ with two terminals in an energy-efficient way. Furthermore, ternary memory can be of utility for highly quantified deep neural networks.

In this study, a VCMA-based and skyrmion-mediated ternary memory system using a single MTJ with two terminals is presented. In addition to the standard "up" and "down" ferromagnetic states of the two-state MRAM system, the third state in the proposed ternary memory system is a skyrmion state. In our system, the skyrmion state exhibits a conductance roughly equal to the average of the highest ("up" ferromagnetic state) and lowest ("down" ferromagnetic state) conductance values which is discussed in the results and discussions section in details. As a result, the skyrmion-mediated memory can be viewed as an almost balanced ternary memory, with resistance states of +1 (ferromagnetic up),  $\sim 0$  (skyrmion), and -1 (ferromagnetic down). Here we note that the magnetization of the reference layer is considered to be pinned in the upward direction. Skyrmions are topologically protected states that offer nanoscale size, high velocity, and low depinning current density [37-39]. These spin textures are usually used in racetrack memory devices [38, 40, 41], but in this study, we propose the usage of a skyrmion in a confined structure like the MTJ. Our group has theoretically shown that switching between the ferromagnetic and skyrmion states in the MTJ's free layer can be done using VCMA at 0 K [42], and also experimentally shown that skyrmions can be created and annihilated in a thin film using VCMA [43]. However, the creation and annihilation of skyrmions at room temperature in a confined structure has not been reported yet. This study theoretically demonstrates that a dense and energy-efficient ternary memory can be implemented by alternating between the three states (ferromagnetic up, ferromagnetic down, and skyrmion as shown in Fig. 1(b)) using VCMA in a patterned 100 nm nanodot in the presence of thermal noise at room temperature. We have shown in other work that such skyrmion based VCMA two-state memory can be scaled to  $< 50$  nm [44,45] which suggests that this approach also has the potential for scalable ternary memory.

The proposed three state memory system can also be used for implementing neuromorphic computing devices, particularly as quantized synaptic weights for deep neural networks (DNN). The demand for neuromorphic computing is growing rapidly due to its ability to handle training and inference tasks in energy-limited environments like edge devices [46-48]. In DNN, the aspect that requires the most time and energy is the vector-matrix multiplication operation [49]. In-memory computing offers a more efficient and low-energy solution to this challenge [48]. The previously mentioned non-volatile memory types, such as magnetoresistive memory [50, 51, 52], flash memory [53], resistive memory [54,55], and phase-change memory [56, 57], have been also shown to be useful in performing multiply-accumulate operations commonly found in artificial neural networks [58]. Of these, magnetoresistive memory has been extensively researched for its high endurance, low energy requirements for reading and writing, non-volatility, and compatibility with CMOS technology [51, 59]. Recently, it has been demonstrated that use of three or five-state domain wall based quantized synaptic weights in deep neural networks can perform recognition tasks with an accuracy comparable to that of floating-point precision synaptic weight based DNNs with low energy consumption [51]. However, writing multiple states in domain wall-based racetrack devices requires a lot of space. In this study, we also discuss that our proposed three-state memory system, implemented in a two-terminal MTJ, allows for the potential implementation of quantized synaptic weights with a

comparable energy consumption to domain wall-based DNNs, but with significantly less space requirements.

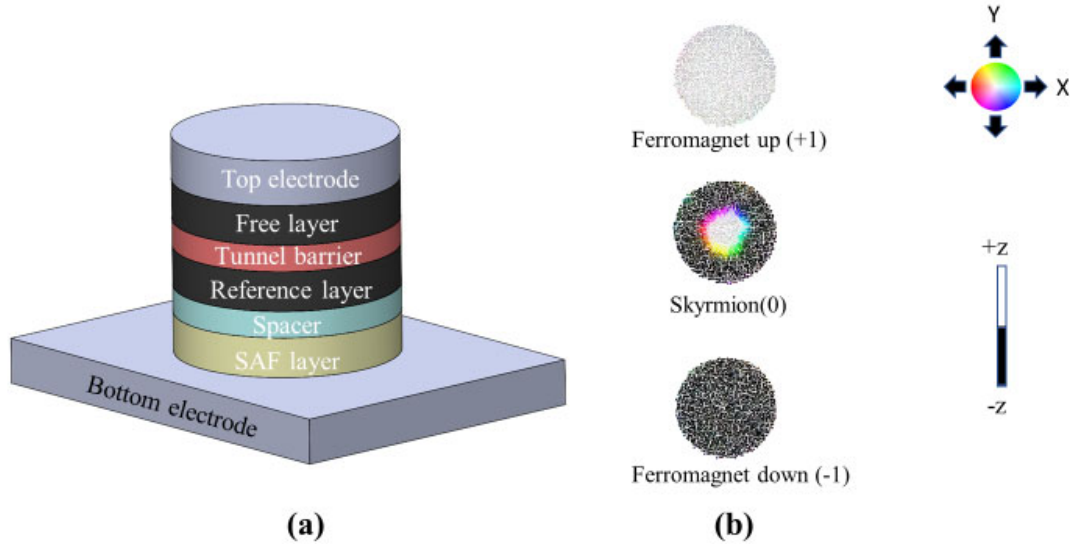


Figure 1. (a) Schematic of a magnetic tunnel junction with different constituent layers. (b) Ferromagnetic up, skyrmion and ferromagnetic down states represent +1, ~0, -1 states, respectively of the proposed ternary memory.

## Results and Discussion

There are three different switching operations that are primarily carried out: switching from a ferromagnet (+1/-1) to a skyrmion state (0), switching from a skyrmion (0) to a ferromagnet state (+1/-1), and switching from one ferromagnet (+1/-1) to another (-1/+1). Here we note that the reference layer is magnetized in the upward direction in the p-MTJ. Therefore, the ferromagnetic up and down state has the highest and lowest conductance, respectively, while the skyrmion state has an intermediate conductance between the highest and lowest [60], which is nearly half of the combined conductance in the case of skyrmions with equal number of up and down spins. This allows the execution of all six interconversions needed to implement a three-state memory. However, as shown in Fig. 2, eight situations occur while performing switching operations.

In case A, switching from ferromagnetic up (+1) to skyrmion state (0) is performed. For performing this switching operation, the ferromagnetic up state is relaxed for 1 ns and perpendicular magnetic anisotropy (PMA) energy is reduced from  $2250 \mu\text{J}/\text{m}^2$  to  $1575 \mu\text{J}/\text{m}^2$  in 0.1 ns by applying a +1 V pulse. Here, we note that it has been previously experimentally observed that positive voltage pulse reduces PMA while negative voltage pulse increases PMA [43, 61]. When the PMA is reduced, the presence of Dzyaloshinskii-Moriya interaction (DMI) field in the ferromagnetic free layer creates a skyrmion state of polarity -1. Here we note that the skyrmion polarity can be defined as  $p = [m_z(r = \infty) - m_z(r = 0)]/2$  [62]. Therefore, skyrmion with boundary (core) pointing down (up) and core (boundary) pointing up(down) has polarity -1 (+1). We observe that when the PMA is reduced from the ferromagnetic up state, a skyrmion of polarity -1 is created because the boundary spins tilt in the opposite direction from the core spins and the core spins are in their starting spin orientation. The voltage pulse is applied for 0.3 ns and subsequently withdrawn in 0.1 ns to restore the initial PMA of  $2250 \mu\text{J}/\text{m}^2$ . We observe that the skyrmion state is stabilized after the withdrawal

of the voltage pulse. Thus, by applying and subsequently withdrawing a +1 V pulse, a skyrmion state (0) can be created and stabilized starting from a ferromagnetic up state (+1).

In case B, we start from a ferromagnetic down state (-1) and when PMA is reduced in 0.1 ns by applying a +1 V pulse, a skyrmion of polarity +1 is created. The skyrmion produced in this instance has the opposite polarity of the one produced in case A because we start from the opposite ferromagnetic state, the ferromagnetic down state. Thus, switching from ferromagnetic down to skyrmion state can be accomplished in a single step similar to case A.

In case C, ferromagnetic up state is switched to ferromagnetic down state. This is a two-step operation. First, a +1 V pulse is applied to reduce the PMA and create a skyrmion state. The created skyrmion has core oriented in the upward direction and boundary in the downward direction. When a -1V pulse is applied to increase the PMA from  $2250 \mu\text{J}/\text{m}^2$  to  $2925 \mu\text{J}/\text{m}^2$  in 0.1 ns, the skyrmion annihilates to the ferromagnetic down state following the skyrmion's downward oriented boundary spins. This switching is deterministic since ferromagnetic up state is switched to ferromagnetic down state through an intermediate skyrmion state which has downward oriented boundary spin and the skyrmion annihilates to ferromagnetic down state following the boundary spins' orientation. We can see from Fig. 2 that the ferromagnetic down state is stable after the PMA is restored by withdrawing the +1V pulse.

Similarly, in case D, ferromagnetic down state is switched to ferromagnetic up state through an intermediate skyrmion state. In this case, starting from a ferromagnetic down state, an intermediate skyrmion with boundary spin in the upward direction and core in the downward direction is created by applying +1V pulse and subsequently the skyrmion is annihilated to ferromagnetic up state by applying -1V pulse. Therefore, writing -1/+1 to +1/-1 is a two-step operation where a positive and a negative voltage pulse is applied sequentially.

Writing from skyrmion to ferromagnet can be one step/three step operation. We have seen in case C and case D that while switching from one ferromagnetic to other ferromagnetic state through an intermediate skyrmion state, the skyrmion state annihilates to ferromagnetic state following the skyrmion state's boundary spin orientation. Writing a desired ferromagnetic state from a skyrmion state can be a one-step or three-step operation depending on the skyrmion polarity because we can't tell the skyrmion's polarity from its magnetoresistance value. For example, if the skyrmion has upward oriented boundary spin then it will annihilate to a ferromagnetic up state (case E). But, if the desired state is the downward ferromagnetic state then the ferromagnetic up state is required to be switched by following the similar operations performed in case C and case D.

In case E, we can see that skyrmion with boundary spin in the upward direction can be switched to a ferromagnetic up state by applying a -1V pulse. If the desired state is ferromagnetic down state then a sequential application of +1 V and -1V pulse will switch the ferromagnetic up state to ferromagnetic down state requiring a three- step operation overall which is shown in case F. If the initial state is a skyrmion state with downward boundary spin and a ferromagnetic down state needs to be written, then the application of a +1V pulse completes the switching as shown in case G. If the desired state is ferromagnetic up state then a sequential application of +1V and -1V pulse will be required to switch the ferromagnetic down state to ferromagnetic up state as shown in case H.

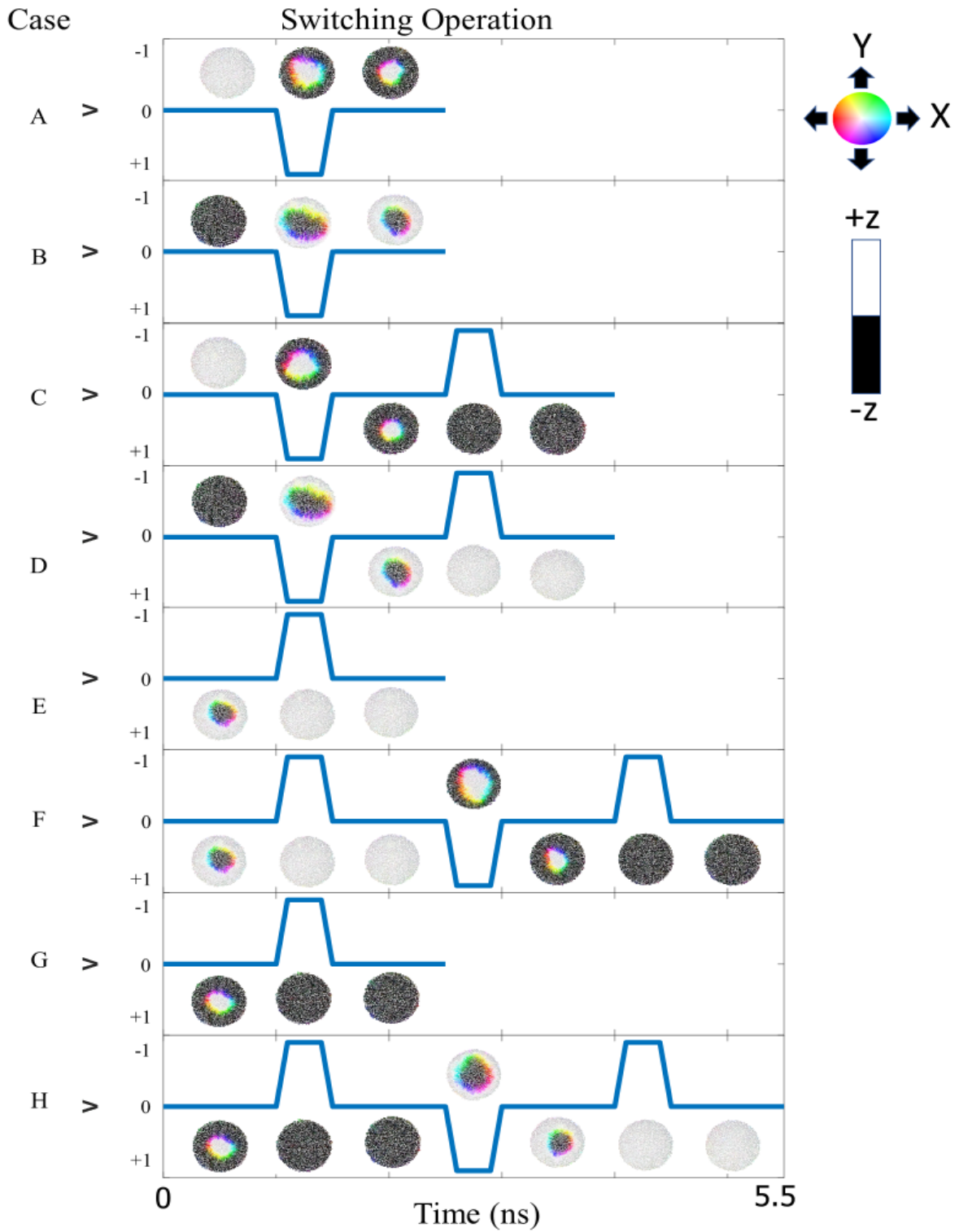


Figure 2. Applied voltage vs time for different switching cases. (The magnetization states for different voltage pulses are shown correspondingly)

We ran simulations for 1000 times to study the switching percentage in each of the eight cases in the presence of room temperature thermal perturbation, and the results are shown in Table 1. On average, switching occurred in ~99% of the cases.

### Energy dissipation:

We calculated the energy required for each switching operation considering all of the reading and writing operations involved. For calculating the energy dissipation, the generalized conductance of the MTJ is considered to have two conductance  $G_1$  and  $G_2$  in parallel as shown in Fig. 3. Therefore, the net conductance of the MTJ is calculated as follows:

$$G_{MTJ} = G_P \left( \frac{A_{RL} - A_{FL/RL}}{A_{RL}} \right) + G_{AP} \frac{A_{FL/RL}}{A_{RL}} \quad (1)$$

where  $A_{RL}$  and  $A_{FL/RL}$  are the area of reference layer (RL) and the area of the free layer (FL) representing the antiparallel region with respect to the reference layer, respectively.

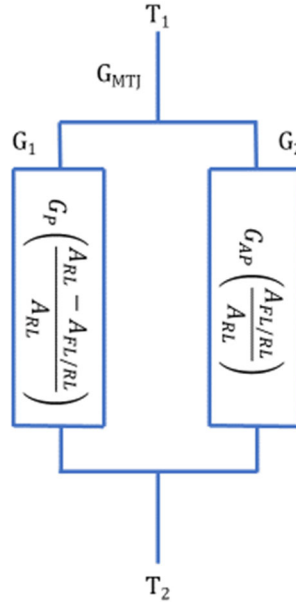


Figure 3. Generalized model of memory state of MTJ

According to the equation 1, the conductance of the parallel and antiparallel states in the MTJ are  $G_P$  and  $G_{AP}$ , respectively. However, when a skyrmion is formed in the FL region with nearly an equal number of spins in the upward and downward direction, it can be assumed that ~50% area of FL is antiparallel to the RL, meaning  $A_{FL/RL} \cong 1/2 A_{RL}$ . Therefore, from equation (1)  $G_{MTJ} \cong \frac{G_P + G_{AP}}{2}$ , which indicates that the conductance of skyrmion state is nearly the average of the conductance of parallel and anti-parallel state. We consider 891.27  $\Omega$  resistance [63] for the parallel orientation of the reference and free layers of the p-MTJ. Considering the TMR ratio 249% [63], therefore, the antiparallel and skyrmion state has 3110.53  $\Omega$  and ~2000.90  $\Omega$  resistance respectively.

While implementing skyrmion-mediated ternary memory, energy is dissipated during both the reading and writing processes that involves  $I_{read}^2 R_{MTJ} t_{read}$  and  $\frac{1}{2} C V_{write}^2$  loss, respectively. To read the states, a 600 mV pulse is applied for 1 ns, while different combinations of read and write pulses are applied to write different states. For example, in case A, the initial and final states are read as ferromagnetic up state, and the skyrmion

state respectively and the energy dissipated for reading is 0.975fJ and 0.886fJ, respectively, thus the total energy dissipated for reading is 1.861fJ. To write the skyrmion state, a +1V is applied for 0.5 ns, resulting in 0.337fJ of switching energy. Therefore, operating case A requires a total of 2.198 fJ of energy. Table 1 shows the energy required for switching from one state to another for all the eight cases. On average, the energy dissipated in writing the three states is 3.19 fJ.

Table 1. Switching percentage and energy dissipation for performing different switching operations

Case	Switching percentage	Write energy (fJ)	Read energy (fJ)	Total energy (fJ)
Case A	98.70	0.337	1.861	2.198
Case B	98.70	0.337	1.739	2.076
Case C	98.80	1.011	2.714	3.725
Case D	99.00	1.011	2.714	3.725
Case E	100	0.337	1.861	2.198
Case F	99.10	1.685	3.600	5.285
Case G	100	0.337	1.739	2.076
Case H	98.9	1.685	3.600	5.285

Previously, nonvolatile multistate memories (3 or 4 states) were proposed using STT or SOT current, and these memories were created by arranging the MTJs in series or parallel configurations [35, 36, 64]. Therefore, implementing multistate memories with STT and SOT current requires at least twice the area of our proposed multistate memory, as shown in Table 2. It is worth noting that in STT/SOT-based multistate memories, two consecutive switching operations are performed to write a single state, resulting in latency issues [64]. Considering the energy required for performing a switching operation with STT current in a single MTJ with a 100 nm diameter, which is the same as the dimension of our proposed device (100 fJ) [65], writing a state in a multistate STT-MRAM would require ~200fJ of energy. On the other hand, although SOT memories require less energy than STT for an MTJ of similar diameter [66] for writing each bit, the requirement of three terminals reduces the density. Thus, our proposed ternary memory achieves at least a 2X improvement in footprint and a ~60X improvement in energy-efficiency compared to STT-based multistate memory.

With an appropriate choice of material parameters, there is still the possibility of reducing the write error rate in the presence of room temperature thermal noise [44,45]. However, the proposed three-state memory system, which achieves ~99% switching accuracy, has the potential to be utilized as quantized synaptic weights for deep neural networks. The previous idea to use three-state domain wall-based quantized synaptic weights achieved similar levels of accuracy during testing as floating-point precision synaptic weights [51]. However, the implementation of the three states requires a large racetrack (600nm× 60nm) [51], and the use of five terminals reduces the density significantly. Our proposed three-state memory system, which uses a single two-terminal MTJ, provides a way to implement quantized synaptic weights

that consume similar amounts of energy as domain wall-based DNNs, but with significantly less space requirement ( $\sim 4.5$  times less space for the MTJ alone) as shown in Table 2.

Table 2. Comparison of different multistate systems

	STT-based two state memory	STT-based multistate memory	DW-based stochastic multistate	Skyrmion-mediated ternary memory
Number of terminals	2	2	$\geq 4$ [51, 64]	2
Area	X	2X [64]	$\sim 4.5X$ [51]	X
Energy	100 fJ [65]	$\sim 200$ fJ	$\sim 3$ fJ [51]	$\sim 3$ fJ

In summary, we showed that a novel skyrmion-mediated ternary memory can be implemented in a p-MTJ in the presence of room temperature thermal noise. We also showed that our proposed ternary memory achieves at least a 2X improvement in footprint and a  $\sim 60X$  improvement in energy-efficiency respectively compared to STT-based multistate memory. By utilizing energy-efficient VCMA switching mechanism and employing a two-terminal MTJ device, our proposed memory design allows for the implementation of three distinct states within a single MTJ, thereby increasing both the cell density and the density of the peripheral circuit. Previously, it has also been theoretically shown that skyrmions can be scaled down to  $\sim 20$  nm in a circular patterned nanodot [45], which could lead to even greater memory density in the future. Furthermore, three state synapses can be built with comparable energy costs and reduced space requirements ( $\sim 4.5$  times less area) compared to domain wall-based quantized DNNs.

## Methods

We simulate the magnetization dynamics of the free layer of the circular shaped p-MTJs with a diameter of 100 nm which are discretized into  $50 \times 50 \times 1$  cells to observe the switching between three states and evaluate the switching probability of each switching case. The simulation uses the MuMAX3 program [67] to solve the magnetization dynamics based on Landau-Lifshitz-Gilbert (LLG) equation that is defined as follows:

$$\frac{\partial \vec{m}}{\partial t} = \left( \frac{-\gamma}{1 + \alpha^2} \right) [\vec{m} \times \vec{B}_{eff} + \alpha \{ \vec{m} \times (\vec{m} \times \vec{B}_{eff}) \}] \quad (2)$$

where  $\alpha$  and  $\gamma$  denote the Gilbert damping coefficient and gyromagnetic ratio, respectively.  $\vec{m}$  indicates the normalized magnetization vector with components  $m_x$ ,  $m_y$ , and  $m_z$  along  $x$ ,  $y$ , and  $z$  direction, respectively, which is obtained by normalizing the magnetization vector ( $\vec{M}$ ) with respect to saturation magnetization ( $M_s$ ). The circular shaped free layers are divided into grids with dimensions of  $2\text{nm} \times 2\text{nm} \times 1.5\text{nm}$ , which are much smaller than the exchange length ( $\sqrt{\frac{2A_{ex}}{\mu_0 M_s^2}}$ ). In the LLG equation  $\vec{B}_{eff}$  is the effective magnetic field having the following components:

$$\vec{B}_{eff} = \vec{B}_{demag} + \vec{B}_{exchange} + \vec{B}_{DM} + \vec{B}_{anis} + \vec{B}_{thermal} \quad (3)$$

In equation (3),  $\vec{B}_{demag}$  represents the effective field due to demagnetization energy and  $\vec{B}_{exchange}$  denotes the Heisenberg exchange interaction respectively.

$\vec{B}_{DM}$  is the effective field due to DMI, which is expressed as follows:



$$\vec{B}_{DM} = \frac{2D}{M_s} \left( \frac{\partial m_z}{\partial x}, \frac{\partial m_z}{\partial y}, -\frac{\partial m_x}{\partial x} - \frac{\partial m_y}{\partial y} \right) \quad (4)$$

Where  $D$  represents the DMI constant.

The perpendicular anisotropy ( $\vec{B}_{anis}$ ) is expressed by the following equation:

$$\vec{B}_{anis} = \frac{2K_{u1}}{M_s} (\vec{u} \cdot \vec{m}) \vec{u} \quad (5)$$

where  $K_{u1}$  and  $\vec{u}$  represent the first order uniaxial anisotropy constant and unit vector in the anisotropy direction respectively.

The following equation is used to introduce the thermal field:

$$\vec{B}_{thermal} = \vec{\eta}(step) \sqrt{\frac{2\alpha k_B T}{M_s \gamma \Delta V \Delta t}} \quad (6)$$

where  $T$  is the temperature (K),  $\Delta V$  is the cell volume,  $k_B$  is the Boltzmann constant,  $\Delta t$  is time step and  $\vec{\eta}$  (step) is a random vector from a standard normal distribution. Here, we note that the random vector  $\vec{\eta}$  is independent (uncorrelated) for each of the three Cartesian coordinates and is generated at every time step.

The parameters for Co based magnetic materials are used for the simulation of magnetization dynamics of the skyrmions that are given in Table 3.

Table 3. Material properties

Saturation magnetization ( $M_s$ )	$1.3 \times 10^6$ A/m [68]
Exchange stiffness ( $A_{ex}$ )	$20 \times 10^{-12}$ J/m [69]
DMI	$3.0 \times 10^{-3}$ J/m <sup>2</sup> [70]
Thickness	1.5 nm
Damping coefficient	0.1 [71]
Perpendicular magnetic anisotropy	$2250 \mu\text{J/m}^2$ [72]
VCMA coefficient	$675 \text{ fJ/Vm}$ [72]

## References

- [1] Chen, A. A review of emerging non-volatile memory (NVM) technologies and applications. *Solid-State Electronics*. **125**, 25-38(2016).
- [2] Banerjee, W. Challenges and applications of emerging nonvolatile memory devices. *Electronics*. **9**, 1029 (2020).
- [3] Wang, K. L., Alzate, J. G. and Amiri, P. K. Low-power non-volatile spintronic memory: STT-RAM and beyond. *Journal of Physics D: Applied Physics*, **46**, 074003(2013).

- [4] Lee, H. Y. *et al.* Low power and high speed bipolar switching with a thin reactive Ti buffer layer in robust HfO<sub>2</sub> based RRAM. IEEE International Electron Devices Meeting, 1-4; 10.1109/IEDM.2008.4796677 (2008)
- [5] Burr, G. W. *et al.* Phase change memory technology. *Journal of Vacuum Science & Technology B, Nanotechnology and Microelectronics: Materials, Processing, Measurement, and Phenomena*, **28**, 223-262(2010)
- [6] Valet, T. and Fert, A. Theory of the perpendicular magnetoresistance in magnetic multilayers. *Physical Review B*, **48**, 7099 (1993).
- [7] Moodera, J. S., Kinder, L. R., Wong, T. M., and Meservey, R. Large magnetoresistance at room temperature in ferromagnetic thin film tunnel junctions. *Physical review letters*. **74**, 3273 (1995).
- [8] Amanuma, K *et al.* Capacitor-on-metal/via-stacked-plug (CMVP) memory cell for 0.25/ $\mu\text{m}$  CMOS embedded FeRAM. *International Electron Devices Meeting, Technical Digest (Cat. No. 98CH36217)*, 363-366; 10.1109/IEDM.1998.746375 (1998).
- [9] Jones, R. E. Ferroelectric nonvolatile memories for embedded applications. *Proceedings of the IEEE 1998 Custom Integrated Circuits Conference (Cat. No. 98CH36143)*, 431-438; 10.1109/CICC.1998.695013 (1998).
- [10] Avalanche technology. <https://www.avalanche-technology.com/technology/mram-technology/>
- [11] Slonczewski, J. C. Current-driven excitation of magnetic multilayers. *Journal of Magnetism and Magnetic Materials*. **159**, L1-L7 (1996).
- [12] Berger, L. Emission of spin waves by a magnetic multilayer traversed by a current. *Physical Review B*. **54**, 9353 (1996).
- [13] Liu, L. *et al.* Spin-torque switching with the giant spin Hall effect of tantalum. *Science*. **336**, 555-558 (2012).
- [14] Misba, W. A., Rajib, M. M., Bhattacharya, D. and Atulasimha, J. Acoustic-wave-induced ferromagnetic-resonance-assisted spin-torque switching of perpendicular magnetic tunnel junctions with anisotropy variation. *Physical Review Applied*, **14**, 014088 (2020).
- [15] Shiota, Y. *et al.* Induction of coherent magnetization switching in a few atomic layers of FeCo using voltage pulses. *Nature materials*. **11**, 39-43 (2012).
- [16] Amiri, P. K. and Wang, K. L. Voltage-controlled magnetic anisotropy in spintronic devices. *Spin*. **2**, 03, 1240002 (2012).
- [17] Wang, W.G., Li, M., Hageman, S. and Chien, C.L. Electric-field-assisted switching in magnetic tunnel junctions. *Nature materials*. **11**, 64-68 (2012).
- [18] Maruyama, T. *et al.* Large voltage-induced magnetic anisotropy change in a few atomic layers of iron. *Nature nanotechnology*. **4**, 158-161 (2009).
- [19] D'Souza, N., Salehi Fashami, M., Bandyopadhyay, S. and Atulasimha, J. Experimental clocking of nanomagnets with strain for ultralow power Boolean logic. *Nano letters*. **16**, 1069-1075 (2016).
- [20] Ralph, D.C. and Stiles, M.D. Spin transfer torques. *Journal of Magnetism and Magnetic Materials*. **320**, 1190-1216 (2008).

- [21] Cui, J. *et al.* A method to control magnetism in individual strain-mediated magnetoelectric islands. *Applied Physics Letters*. **103**, 232905 (2013).
- [22] Biswas, A.K., Ahmad, H., Atulasimha, J. and Bandyopadhyay, S. Experimental demonstration of complete 180 reversal of magnetization in isolated co nanomagnets on a pmn-pt substrate with voltage generated strain. *Nano letters*. **17**, 3478-3484 (2017).
- [23] Zhao, Z. *et al.* Giant voltage manipulation of MgO-based magnetic tunnel junctions via localized anisotropic strain: A potential pathway to ultra-energy-efficient memory technology. *Applied Physics Letters*. **109**, 092403 (2016).
- [24] Al-Rashid, M.M., Bandyopadhyay, S. and Atulasimha, J. Dynamic error in strain-induced magnetization reversal of nanomagnets due to incoherent switching and formation of metastable states: a size-dependent study. *IEEE Transactions on Electron Devices*, **63**, 3307-3313 (2016).
- [25] Roy, K., Bandyopadhyay, S. and Atulasimha, J. Hybrid spintronics and straintronics: A magnetic technology for ultra low energy computing and signal processing. *Applied Physics Letters*. **99**, 063108 (2011).
- [26] Ahmad, H., Atulasimha, J. and Bandyopadhyay, S. Reversible strain-induced magnetization switching in FeGa nanomagnets: Pathway to a rewritable, non-volatile, non-toggle, extremely low energy straintronic memory. *Scientific reports*. **5**, 1-7 (2015).
- [27] Bandyopadhyay, S., Atulasimha, J. and Barman, A. Magnetic straintronics: Manipulating the magnetization of magnetostrictive nanomagnets with strain for energy-efficient applications. *Applied Physics Reviews*. **8**, 041323 (2021).
- [28] Weisheit, M. *et al.* Electric field-induced modification of magnetism in thin-film ferromagnets. *Science*. **315**, 349-351(2007).
- [29] Niranjana, M.K., Duan, C.G., Jaswal, S.S. and Tsymbal, E.Y. Electric field effect on magnetization at the Fe/MgO (001) interface. *Applied Physics Letters*, **96**, 222504 (2010).
- [30] Heron, J.T. *et al.* Deterministic switching of ferromagnetism at room temperature using an electric field. *Nature*, **516**, 370-373 (2014).
- [31] Atulasimha, J. and Bandyopadhyay, S. Bennett clocking of nanomagnetic logic using multiferroic single-domain nanomagnets. *Applied Physics Letters*. **97**, 173105 (2010).
- [32] Shiota, Y. *et al.* Evaluation of write error rate for voltage-driven dynamic magnetization switching in magnetic tunnel junctions with perpendicular magnetization. *Applied Physics Express*. **9**, 013001 (2015).
- [33] Grezes, C. *et al.* Ultra-low switching energy and scaling in electric-field-controlled nanoscale magnetic tunnel junctions with high resistance-area product. *Applied Physics Letters*. **108**, 012403 (2016).
- [34] Nowak, J. J. *et al.* Dependence of voltage and size on write error rates in spin-transfer torque magnetic random-access memory. *IEEE Magnetics Letters*. **7**, 1-4 (2016).
- [35] Ishigaki, T. *et al.* A multi-level-cell spin-transfer torque memory with series-stacked magnetotunnel junctions. *Symposium on VLSI Technology*. 47-48; 10.1109/VLSIT.2010.5556126 (2010).
- [36] Kim, Y., Fong, X., Kwon, K.W., Chen, M.C. and Roy, K. Multilevel spin-orbit torque MRAMs. *IEEE Transactions on Electron Devices*. **62**, 561-568 (2014).

- [37] Roessler, U.K., Bogdanov, A.N. and Pfleiderer, C. Spontaneous skyrmion ground states in magnetic metals. *Nature*. **442**, 797–801 (2006).
- [38] Fert, A., Cros, V. and Sampaio, J. Skyrmions on the track. *Nat. Nanotechnol.* **8**, 152–156 (2013).
- [39] Komineas, S. and Papanicolaou, N. Skyrmion dynamics in chiral ferromagnets. *Physical Review B*, **92**, 064412 (2015).
- [40] Tomasello, R., Martinez, E., Zivieri, R., Torres, L., Carpentieri, M. and Finocchio, G. A strategy for the design of skyrmion racetrack memories. *Sci. Rep.* **4**, 1–7 (2014).
- [41] Iwasaki, J., Mochizuki, M. and Nagaosa, N. Current-induced skyrmion dynamics in constricted geometries. *Nat. Nanotechnol.* **8**, 742–747 (2013).
- [42] Bhattacharya, D., Al-Rashid, M.M. and Atulasimha, J. Voltage controlled core reversal of fixed magnetic skyrmions without a magnetic field. *Scientific reports*. **6**, 1-6 (2016).
- [43] Bhattacharya, D. *et al.* Creation and annihilation of non-volatile fixed magnetic skyrmions using voltage control of magnetic anisotropy. *Nature Electronics*. **3**, 539-545 (2020).
- [44] Rajib, M.M., Al Misba, W., Bhattacharya, D., Garcia-Sanchez, F. and Atulasimha, J. Dynamic skyrmion-mediated switching of perpendicular MTJs: feasibility analysis of scaling to 20 nm with thermal noise. *IEEE Transactions on Electron Devices*. **67**, 3883-3888 (2020).
- [45] Rajib, M.M., Misba, W.A., Bhattacharya, D. and Atulasimha, J. Robust skyrmion mediated reversal of ferromagnetic nanodots of 20 nm lateral dimension with high  $M_s$  and observable DMI. *Scientific reports*, **11**, 20914 (2021).
- [46] Schuman, C. D. *et al.* Opportunities for neuromorphic computing algorithms and applications. *Nature Computational Science*. **2**, 10-19 (2022).
- [47] Rajib, M.M., Al Misba, W., Chowdhury, M.F.F., Alam, M.S. and Atulasimha, J. Skyrmion based energy-efficient straintronic physical reservoir computing. *Neuromorphic Computing and Engineering*. **2**, 044011 (2022).
- [48] Li, C. *et al.* Analogue signal and image processing with large memristor crossbars. *Nature electronics*. **1**, 52-59 (2018).
- [49] Hu, M. *et al.* Dot-product engine for neuromorphic computing: Programming 1T1M crossbar to accelerate matrix-vector multiplication. *Proceedings of the 53rd annual design automation conference*. 1-6; 10.1145/2897937.2898010 (2016).
- [50] Bhowmik, D. *et al.* On-chip learning for domain wall synapse based fully connected neural network. *Journal of Magnetism and Magnetic Materials*. **489**, 165434 (2019).
- [51] Al Misba, W., Lozano, M., Querlioz, D. and Atulasimha, J. Energy efficient learning with low resolution stochastic domain wall synapse for deep neural networks. *IEEE Access*. **10**, 84946-84959 (2022).
- [52] Leonard, T. *et al.* Shape-Dependent Multi-Weight Magnetic Artificial Synapses for Neuromorphic Computing. *Advanced Electronic Materials*, **8**, 2200563 (2022).
- [53] Wang, P. *et al.* Three-dimensional NAND flash for vector–matrix multiplication. *IEEE Transactions on Very Large Scale Integration (VLSI) Systems*. **27**, 988-991 (2018).

- [54] Yao, P. et al. Fully hardware-implemented memristor convolutional neural network. *Nature*. **577**, 641-646 (2020).
- [55] Ielmini, D. and Wong, H.S.P. In-memory computing with resistive switching devices. *Nature electronics*. **1**, 333-343 (2018).
- [56] Gallo, M. L. et al. Mixed-precision in-memory computing. *Nature Electronics*, **1**, 246-253 (2018).
- [57] Ambrogio, S. et al. Equivalent-accuracy accelerated neural-network training using analogue memory. *Nature*. **558**, 60-67 (2018).
- [58] Jung, S. et al. A crossbar array of magnetoresistive memory devices for in-memory computing. *Nature*. **601**, 211-216 (2022).
- [59] Wong, H. S. P. and Salahuddin, S. Memory leads the way to better computing. *Nature nanotechnology*. **10**, 191-194 (2015).
- [60] Zhang, X. et al. Skyrmions in magnetic tunnel junctions. *ACS applied materials & interfaces*. **10**, 16887-16892 (2018).
- [61] Amiri, P. K. et al. Electric-field-controlled magnetoelectric RAM: Progress, challenges, and scaling. *IEEE Transactions on Magnetics*. **51**, 1-7 (2015).
- [62] Wang, X. S., Yuan, H. Y. and Wang, X. R. A theory on skyrmion size. *Communications Physics*. **1**, 31 (2018).
- [63] Wang, M. et al. Current-induced magnetization switching in atom-thick tungsten engineered perpendicular magnetic tunnel junctions with large tunnel magnetoresistance. *Nature communications*. **9**, 671 (2018).
- [64] Cao, Q. et al. Nonvolatile multistates memories for high-density data storage. *ACS Applied Materials & Interfaces*. **12**, 42449-42471 (2020).
- [65] Chen, A. et al. Full voltage manipulation of the resistance of a magnetic tunnel junction. *Science Advances*, **5**, eaay5141 (2019).
- [66] Sura, A. and Nehra, V. Performance comparison of single level STT and SOT MRAM cells for cache applications. *25th International Symposium on VLSI Design and Test (VDATE)*. IEEE. 1-4; 10.1109/VDATE53777.2021.9601129 (2021).
- [67] Vansteenkiste, A. et al. The design and verification of MuMax3. *AIP advances*. **4**, 107133 (2014).
- [68] Concaa, A. et al. Low spin-wave damping in amorphous Co<sub>40</sub>Fe<sub>40</sub>B<sub>20</sub> thin films. *Journal of Applied Physics*. **113**, 213909 (2013).
- [69] Devolder, T. et al. Exchange stiffness in ultrathin perpendicularly magnetized CoFeB layers determined using the spectroscopy of electrically excited spin waves. *Journal of Applied Physics*. **120**, 183902 (2016).
- [70] Cao, A. et al. Enhanced interfacial Dzyaloshinskii—Moriya interactions in annealed Pt/Co/MgO structures. *Nanotechnology*. **31**, 155705 (2020).
- [71] Sajitha, E. P. et al. Magnetization dynamics in CoFeB buffered perpendicularly magnetized Co/Pd multilayer. *IEEE transactions on magnetics*. **46**, 2056-2059 (2010).

[72] Kato, Y. *et al.* Giant voltage-controlled magnetic anisotropy effect in a crystallographically strained CoFe system. *Applied Physics Express*. **11**, 053007 (2018).

### **Acknowledgements**

M. M. R. and J. A. would like to acknowledge US National Science Foundation CISE SHF Small grant # 1909030. N.B., R. K. R. and B. K. K would like to acknowledge Science and Engineering Research Board (SERB), Department of Science and Technology, Government of India under Grant CRG/2019/004551 for providing the funding to carry out the research work.

### **Competing interests**

The authors declare no competing interests.